The configurational contribution to the segmental orientation in network chains subject to perturbation by the excluded volume effect

Ivet Bahar and Wayne L. Mattice

Department of Chemical Engineering, Bogazici University, 80815 Bebek, Istanbul, Turkey and Institute of Polymer Science, The University of Akron, Akron, Ohio 44325

The influence of the excluded volume effect on the configurational contribution to the segmental orientation in network chains is evaluated using rotational isomeric state theory. The chains used are rotational isomeric state models for polyethylene, poly(vinyl bromide), and poly(vinyl chloride), as well as some simplistic models for polyethylene. The long-range interactions may be attractive or repulsive. Chain expansion in response to the excluded volume effect is accompanied by an increase in orientational entropy (or disorder), which is apparent from the decrease in the absolute magnitude of the orientation function. Conversely, any tendency for orientation in a preferred direction is enhanced by chain contraction.

I. INTRODUCTION

Spectroscopic methods such as infrared dichroism,[2] H-NMR, fluorescence polarization, and wide-angle x-ray scattering permit precise determination of the segmental orientation in deformed amorphous networks. A quantitative measure of the degree of orientation in deformed amorphous networks is the orientation function S, defined as

$$S = (3\langle \cos^2 \theta \rangle - 1)/2 , \qquad (1)$$

where the angle brackets denote the ensemble average over all chains and/or bonds, depending on the experimental procedure, and θ is the angle between the experimentally investigated vectorial quantity rigidly embedded in the network chain and a laboratory fixed reference direction which may be conveniently chosen as that of the macroscopic applied extension. For random orientation $\langle \cos^2 \theta \rangle = 1/3$ and hence $S = 0$. A positive or negative value for S indicates a preference in the reference direction or the opposite, respectively. For three mutually perpendicular vectors, such as the x, y, and z components of bond-based coordinate systems, at least one of the orthonormal vectors is expected to exhibit negative orientation with respect to the preferred direction because the three average squared cosines must sum up to unity.

The usual procedure for calculating S involves two steps: first a configurational average $\langle \cos^2 \theta \rangle_r$ is evaluated for a chain with fixed end-to-end vector r. Here the subscript r indicates the constancy of r. Then an ensemble average over a family of chains varying in r is considered. From a recent theory of segmental orientation developed by Erman and Monnerie,[1] the resulting expression may be formulated as the product of two distinct terms referred to as the configurational factor and the strain function. The strain function reflects the deformation of the network chains as a result of macroscopic strain in conformity with the theory of rubber elasticity. The expression for the strain function was refined[1] by removing the assumption of affine deformation which is common to previous related treatments, and using instead the constrained junction theory of rubber elasticity.

As to the configurational factor, it may be evaluated on the basis of hypothetical models, such as the freely jointed chain, or using more realistic approaches, such as the rotational isomeric state (RIS) formalism. The RIS model was recently used for the evaluation of the configurational factor and the influence of various conformational and structural characteristics on segmental orientation.[2] The orientation of a given vector was found to depend strongly on its specific direction with respect to the motional bond-based reference frame and the length of the network chain to which it is rigidly embedded. Calculations were performed for unperturbed polyethylene chains, using the matrix generation techniques of the RIS model.

The configuration-dependent properties usually evaluated by the RIS model are valid for unperturbed chains only, i.e., in the absence of the excluded volume effect. Recently, Gao and Weiner[3] drew attention to the influence of volume exclusion on segmental orientation in network chains. From a molecular dynamics simulation of freely jointed chains subject to a Lennard-Jones repulsive potential, the excluded volume is found to have a significant effect on segmental orientation and to lead to negative orientation for sufficiently contracted chains.

A more realistic estimation of the effect of volume exclusion on segmental orientation may be carried out through Monte Carlo simulations of real chains. Such calculations may be viewed as semiexperiments that provide insights into real chain behavior. In a series of papers, simulations with RIS models were performed by Mattice and collaborators[4,5] to investigate the intramolecular excluded volume effect on various configuration-dependent properties of polymer chains, such as the dipole moments and optical anisotropies. Both simplistic models and realistic polymers, such as polyethylene (PE), polyvinyl chloride (PVC), polyvinyl bromide (PVB), polystyrene, and its halogenated derivatives were generated. Initially, long-range interactions were introduced through the use of hard-sphere repulsive interaction potentials.[4] This approach was recently modified,[5] so that both repulsive and attractive intramolecular interactions are incorporated, thus permitting expansion or contraction of the chain. The same scheme is adopted in the present study

to investigate the manner in which the imposition of long-range interactions affects the configurational factor of the orientation function for a chain with fixed r. In Sec. II, the theory of segmental orientation is briefly outlined. Section III describes the simulation method and reports the numerical results of the calculations, which are discussed in Sec. IV.

II. THEORY

Consider a chain consisting of n skeletal bonds with one end fixed at the origin O of a laboratory-fixed coordinate system $OXYZ$ and the other at a location r from the origin. The components of r along the laboratory-fixed axes are x_r, y_r, and z_r. Let m be a unit vector rigidly affixed to the chain at a specific location. The chain may assume all configurations consistent with the end-to-end vector r, and consequently m assumes various orientations with respect to the laboratory-fixed frame as the chain undergoes conformational transitions. Let θ be the angle between m and the X axis of the frame $OXYZ$. The X axis may be identified as the direction of stretch for chains under uniaxial tension. The average orientation of m with respect to the X axis may be represented by the second moment $\langle \cos^2 \theta \rangle_r$, which may be written in series as[6,7]

$$\langle \cos^2 \theta \rangle_r = 1/3 + D_0(3x_r^2 - r^2)/\langle r^2 \rangle_0 + \cdots, \quad (2)$$

where averages with subscript zero refer to ensembles of unperturbed chains, free of an external stress, and D_0 is the configurational factor of the orientation function, defined[1] as

$$D_0 = (3\langle r^2 \cos^2 \Phi_m \rangle_0 / \langle r^2 \rangle_0 - 1)/10. \quad (3)$$

Here Φ_m is the angle between the end-to-end vector r and the unit vector m. In Eq. (2) the first term is the value for random or isotropic orientation of m. Any departure from random orientation resulting from the inherent anisotropic character of segmental motion is accounted for by the additional terms in the series. The second term represents contributions of the order of $1/n$. Terms of the order of $1/n^2$ (and higher), which are present in the original treatment of Nagai,[6] are omitted in the present study as their relative contribution is expected to be negligibly small for $n \geqslant 40$.

When the end-to-end vector r coincides with the X axis, Eq. (2) reduces to

$$\langle \cos^2 \theta \rangle_r = 1/3 + \beta_2 r^2 / \langle r^2 \rangle_0 + \cdots, \quad (4)$$

where

$$\beta_2 = (3\langle r^2 \cos^2 \Phi_m \rangle_0 / \langle r^2 \rangle_0 - 1)/5 \quad (5)$$

following the notation of Ref. 8. For freely jointed chains, the equation equivalent to Eq. (4) is

$$\langle \cos^2 \theta \rangle_r = 1 - (2r/nl)/L^*(r/nl)$$

$$= 1/3 + (2/5)(r/nl) + (24/175)(r/nl)^3 + \cdots, \quad (6)$$

where L^* is the inverse Langevin function and l is the bond length.

Combining Eqs. (1) and (2), the orientation function S_r for m in a chain subject to constancy of r is

$$S_r = (3D_0/2)[(2x_r^2 - y_r^2 - z_r^2)/\langle r^2 \rangle_0]. \quad (7)$$

For an ensemble of chains with various r, using the relationships $r^2 = x_r^2 + y_r^2 + z_r^2$ and $\langle x_r^2 \rangle_0 = \langle y_r^2 \rangle_0 = \langle z_r^2 \rangle_0 = \langle r^2 \rangle_0/3$, Eq. (7) becomes

$$S = D_0[\Lambda_x^2 - (\Lambda_y^2 - \Lambda_z^2)/2], \quad (8)$$

where Λ_x^2, Λ_y^2, and Λ_z^2 are the principal components of the molecular deformation tensor Λ^2. Λ_x^2 is defined by the ratio $\langle x_r^2 \rangle_0 / \langle x_r^2 \rangle$, where $\langle x_r^2 \rangle$ refers to an ensemble of chains deformed by an external stress. The term in brackets in Eq. (8) was further improved[1] by including the effect of the local distortion of the junction constraint domains in the network chains. Also the configurational factor D_0 was replaced[1] by

$$D = D_0 + D_{\text{int}}, \quad (9)$$

where D_{int} accounts for the contribution of intermolecular interactions to segmental orientation.

The configurational factor D_0, given by Eq. (3), may be calculated using the RIS model and the related matrix generation techniques, as shown recently.[2] However, for real chains subject to the excluded volume effect, D_0 and consequently S are expected to be influenced by long-range interactions. For perturbed chains, the ensemble averages $\langle r^2 \rangle_0$ and $\langle r^2 \cos^2 \Phi_m \rangle_0$ in Eqs. (2) and (3) are replaced by $\langle r^2 \rangle$ and $\langle r^2 \cos^2 \Phi_m \rangle$. Consequently, using Eq. (7), for chains perturbed by long-range interactions S_{ev} replaces S_r as

$$S_{\text{ev}} = \alpha_{sm}^2 S_r, \quad (10)$$

where α_{sm}^2 is defined as

$$\alpha_{sm}^2 = \{[3\langle r^2 \cos^2 \Phi_m \rangle/\langle r^2 \rangle - 1]\langle r^2 \rangle_0\}/ \{[3\langle r^2 \cos^2 \Phi_m \rangle_0/\langle r^2 \rangle_0 - 1]\langle r^2 \rangle\}. \quad (11)$$

The subscript ev in Eq. (10) refers to the excluded volume effect. In a strict sense, the latter does not necessarily lead to an exclusion of volume or a chain expansion. The contraction of the chain is also possible, depending on the way the interaction potentials are introduced (see sequel). To examine the effect of both repulsive and attractive long-range interactions, the approach outlined in Sec. III is used.

III. SIMULATION

The average quantities of interest in the present study are $\langle r^2 \cos^2 \Phi_m \rangle = \langle (r \cdot m)^2 \rangle$ and $\langle r^2 \rangle$. The unit vector m will be rigidly fixed to the local coordinate frame for bond $n/2 + 2$. Three directions identified with the x, y, and z axes of that local frame are considered. Accordingly, m will be replaced by x, y, and z in the following:

The simulation method proposed in a recent paper[5] is adopted in the present work. A brief outline is given here. Monte Carlo chains are generated using the *a priori* and conditional probabilities for the conformational states of skeletal bonds, based on statistics for unperturbed real chains. The chains are weighted according to the prevailing long-range interaction as follows: Every other atom along the backbone is assigned a van der Waals sphere of radius r^* and the number of n_w of overlapping spheres separated by more than six skeletal bonds are counted to determine the statistical weight of a given configuration. This statistical weight is equal to w^{n_w}, where w is the interaction parameter varying in the interval $0 < w < 1.2$. In particular, $w = 0$ for a hard-

sphere potential, $0 < w < 1$ for a repulsive interaction, $w = 1$ for unperturbed chains, and $w > 1$ for an attractive interaction. The number n_w of overlaps may be varied by suitable choice of r^*, which is in general, expressed in the form r^*/l. From various combinations of r^*/l and w, the response of the second moments $\langle r^2 \rangle$ and $\langle r^2 \cos^2 \Phi_m \rangle$, to the expansion or contraction of the chain, may be found.

Calculations were performed for the following models:

I. Polyethylene (PE) with the rotational isomeric state model described by Abe, Jernigan, and Flory.[9] The bond angle is 112°, the dihedral angles for the *gauche* states are located at $\pm 120°$ from the dihedral angle for the *trans* state and the conformational energies for first- and second-order interactions are 0.5 and 2 kcal/mol, respectively.

II. A simplified polyethylene with independent bonds. This chain differs from the one above in that second-order interactions are ignored.

III. A hypothetical polyethylene-like chain which does not differentiate between *gauche* and *trans* states. This chain has the same geometrical parameters as models I and II, but there are no repulsive first- or second-order interactions.

IV, V, VI. PVB following the RIS model of Saiz *et al.*[10] The fraction of meso dyads p_m equals 0, 0.5, and 1 in the models IV, V, and VI, respectively.

VII, VIII, IX. PVC with the RIS model described by Mark[11] for $p_m = 0, 0.5$, and 1, respectively.

For each model, two independent sets of 100 000 representative Monte Carlo chains with $n = 100$, are generated. The temperature is taken to be 300 K. For model I, computations are repeated for various n in the range $40 \leqslant n \leqslant 200$.

Properties calculated for unperturbed chains are $\langle r^2 \rangle_0$ and the three $\langle r^2 \cos^2 \Phi_m \rangle_0$ with $m = x, y, z$. Division by nl^2 yields the characteristic ratio C_n, and the three C_{nm}, where $C_n = \Sigma C_{nm}$. The resulting C_n and $C_{nm}/C_n = \langle r^2 \cos^2 \Phi_m \rangle_0 / \langle r^2 \rangle_0$ obtained from the two sets for each model chain are listed in Table I. The C_{nm}/C_n are plotted in Fig. 1, as a function of $1/n$ for model I. The data are given in Table II.
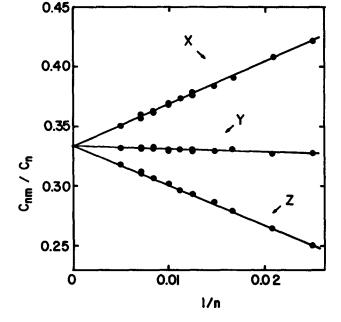

FIG. 1. Values of C_{nx}/C_n, C_{ny}/C_n, and C_{nz}/C_n for unperturbed polyethylene chains as a function of $1/n$. The data plotted are from Table II.

The influence of long-range interactions was analyzed, in analogy to a recently introduced procedure,[5] as follows: The first properties calculated for the perturbed ensembles are $\langle r^2 \rangle$ and $\langle r^2 \cos^2 \Phi_m \rangle$. These properties are combined with the results from the unperturbed ensembles to give three α_{sm}^2, defined by Eq. (11). For each m, the α_{sm}^2 for various combinations of r^*/l and w are plotted as a function of $\langle r^2 \rangle / \langle r^2 \rangle_0 = \alpha_r^2$, as illustrated in Fig. 2 for model I with $n = 100$. The data plotted exhausts all combinations of $r^*/l = 0.6, 1.0, 1.4$, and 1.8, and $w = 0, 0.5, 0.7, 1.04$, and 1.08. The number of distinguishable points in the three panels is

TABLE I. Values of C_n and C_{nm}/C_n for two independent simulations of unperturbed chains with $n = 100$.

Chain	C_n	C_{nx}/C_n	C_{ny}/C_n	C_{nz}/C_n
I	7.509	0.367	0.331	0.302
	7.479	0.369	0.329	0.302
II	4.041	0.353	0.333	0.314
	4.023	0.354	0.333	0.313
III	1.465	0.342	0.328	0.330
	1.463	0.338	0.332	0.329
IV	10.28	0.378	0.260	0.363
	10.29	0.378	0.258	0.364
V	7.721	0.369	0.334	0.297
	7.789	0.370	0.336	0.294
VI	12.60	0.411	0.359	0.230
	12.62	0.411	0.360	0.229
VII	29.68	0.526	0.289	0.184
	29.72	0.525	0.289	0.186
VIII	10.39	0.390	0.337	0.273
	10.32	0.386	0.340	0.274
IX	8.423	0.380	0.347	0.273
	8.432	0.381	0.347	0.271

TABLE II. Values of C_n and C_{nm}/C_n for two independent simulations of unperturbed polyethylene chains.

n	C_n	C_{nx}/C_n	C_{ny}/C_n	C_{nz}/C_n
40	6.780	0.422	0.328	0.250
	6.773	0.421	0.327	0.251
48	6.995	0.408	0.327	0.264
	6.981	0.408	0.327	0.265
60	7.187	0.390	0.331	0.279
	7.163	0.390	0.330	0.280
68	7.287	0.384	0.330	0.286
	7.273	0.384	0.329	0.287
80	7.375	0.379	0.328	0.293
	7.344	0.376	0.331	0.293
88	7.449	0.374	0.330	0.296
	7.416	0.373	0.330	0.297
100	7.509	0.367	0.331	0.302
	7.479	0.369	0.329	0.302
120	7.548	0.361	0.333	0.306
	7.559	0.363	0.331	0.307
140	7.627	0.356	0.332	0.312
	7.640	0.360	0.330	0.310
200	7.727	0.351	0.331	0.317
	7.735	0.350	0.332	0.318

TABLE III. Values of D_m for two independent simulations of perturbed polyethylene chains.

n	D_x	D_y	D_z
40	− 0.55	− 0.83	− 0.53
	− 0.56	− 0.73	− 0.55
48	− 0.49	− 0.44	− 0.49
	− 0.56	− 0.66	− 0.54
60	− 0.55	− 1.35	− 0.51
	− 0.52	− 1.11	− 0.48
68	− 0.44	− 0.40	− 0.48
	− 0.54	− 0.32	− 0.56
80	− 0.39	0.74	− 0.54
	− 0.43	0.04	− 0.46
88	− 0.25	− 0.26	− 0.26
	− 0.66	− 1.04	− 0.62
100	− 0.61	− 2.24	− 0.47
	− 0.58	− 2.08	− 0.40
120	− 0.79	− 10.19	− 0.52
	− 0.55	− 0.25	− 0.57
140	− 0.55	− 2.97	− 0.41
	− 0.50	0.36	− 0.62
200	− 0.76	− 1.36	− 0.68
	− 0.07	1.77	− 0.25

17 or 19, rather than 20, due to overlap of some of the points. The slopes of the three straight lines are − 0.61, − 2.24, and 0.47 for x, y, and z, respectively. Scatter is greatest in the middle panel, for reasons that will become apparent below.

In general, straight lines analogous to those depicted are obtained with $w = 0$, 0.3, 0.5, 0.7, 0.85, 1.05, 1.1, 1.15, 1.2 and $r^*/l = 0.4$, 0.6, 0.8, 1.0, 1.2, 1.4, 1.6, 1.8. The best line is drawn through the points for which $0.9 < \alpha_r^2 < 1.1$. This straight line is constrained to pass through the point $(\alpha_{sm}^2, \alpha_r^2) = (1,1)$. The slope of this straight line is denoted by D_m. Consequently, D_m denotes the initial influence of the perturbation on α_{sm}^2, i.e., $D_m = (\partial \alpha_{sm}^2/\partial \alpha_r^2)$ evaluated at $\alpha_r^2 = 1$. The results for D_m are given in Table III for model I with various n, and in Table IV for all model chains with

TABLE IV. Values of D_m for two independent simulations of chains with $n = 100$.

Chain	D_x	D_y	D_z
I	− 0.49	~ − 200	− 0.16
	− 0.62	+ 22	− 0.84
II	+ 0.03	− 0.18	+ 0.40
	− 0.69	− 2.16	− 0.21
III	− 0.49	− 0.98	− 1.74
	− 0.68	− 0.96	− 1.37
IV	− 0.42	− 1.28	− 0.44
	− 0.50	− 0.62	− 0.50
V	− 0.70	− 0.32	− 0.58
	− 0.56	− 0.46	− 0.54
VI	− 0.71	− 1.13	− 0.60
	− 0.73	− 0.99	− 0.66
VII	− 0.54	+ 0.07	− 0.50
	− 0.53	− 0.48	− 0.53
VIII	− 0.44	− 0.23	− 0.38
	− 0.66	− 0.29	− 0.58

TABLE V. Averages of selected entries from Table III.

n	$\langle D_x \rangle$	SD	$\langle D_y \rangle$	SD	$\langle D_z \rangle$	SD
40–200	− 0.52	0.15	− 1.17	2.31	− 0.50	0.07
40–80	− 0.50	0.06	− 0.51	0.56	− 0.51	0.03
88–200	− 0.53	0.21	− 1.83	3.08	− 0.48	0.12

$n = 100$. In general, negative values are obtained for D_m. There is no obvious trend for D_m with n, for $40 \leqslant n \leqslant 200$.

For model I, the averages of D_m over various ranges of n and the corresponding standard deviations are listed in Table V. The $\langle D_z \rangle$ are virtually indistinguishable from the $\langle D_x \rangle$, both being approximately equal to − 0.5. The standard deviation increases with n, as expected, because all sets contain the same number of chains. The values for D_y are chaotic and the standard deviations are enormous. The origin of the large standard deviation for D_y is apparent upon inspection of the data in Table II. Since C_{ny}/C_n is very close to 1/3, the value of $3\langle r^2 \cos^2 \Phi_y \rangle_0/\langle r^2 \rangle_0$ is very close to 1. Consequently, very small uncertainties in the evaluation of $\langle r^2 \cos^2 \Phi_y \rangle_0/\langle r^2 \rangle_0$ and $\langle r^2 \cos^2 \Phi_y \rangle/\langle r^2 \rangle$ from the unperturbed and perturbed ensembles can produce enormous fluctuations in D_y. The values of D_x and D_z are more easily established by the simulations than are the values of D_y because C_{nx}/C_n and C_{nz}/C_n differ from 1/3 by a larger amount than does C_{ny}/C_n. This feature is common to the other model chains as well, as may be observed from the results in Table IV, in relation to Table I.

IV. DISCUSSION AND CONCLUSION

From the analysis of the results for perturbed chains in Tables I and II, it may be seen that the two values for C_n at a particular chain never differ by more than 0.9%. Also, the percent difference between C_{nm}/C_n values obtained from the two sets is always lower than 1.2%. Thus the two independent sets of 100 000 Monte Carlo chains satisfactorily represent the orientational behavior of unperturbed chains.

In the present study, the label characterized by the vector m is assumed to be rigidly embedded in the local frame of bond $n/2 + 2$. It should be noted that, from recent calculations[2] for $n = 100$, the configurational factor D_0 is found to be almost independent of i in the interval $25 \leqslant i \leqslant 75$, where i is the index of the local frame to which m is attached. Thus the exact location of m is immaterial as long as it is in this interval.

The C_{nm}/C_n values have the expected limiting value of 1/3, regardless of the direction of m within the local frame, as can be verified by extrapolation of the plot of C_{nm}/C_n vs $1/n$, in Fig. 1. Thus for long chains, the orientational correlations between r and m vanish such that $\langle r^2 \cos^2 \Phi_m \rangle_0 = \langle r^2 \rangle_0 \langle \cos^2 \Phi_m \rangle_0 = 1/3 \langle r^2 \rangle_0$, as n goes to infinity. As a result, the configurational factor D_0 in Eq. (3) equates to zero and, as expected, $\langle \cos^2 \theta \rangle_r$ assumes its value for random orientation of m, i.e., 1/3, as apparent from Eq. (2), leading to $S = 0$.

Results for polyethylene (model I) compare favorably with those obtained[2] by an analytical method. The ratio

$\langle r^2 \cos^2 \Phi_m \rangle_0 / \langle r^2 \rangle_0$ is a measure of the orientational correlation between r and m. In fact, the orientation function for m and r may be expressed as $S = (3\langle r^2 \cos^2 \Phi_m \rangle_0 / \langle r^2 \rangle_0 - 1)/2$. Accordingly, there is positive orientational correlation between r and m when $m = x$. A weaker, but still positive, orientational correlation exists between r and y, as well. However, for m along the z axis of the local frame, the ratio $\langle r^2 \cos^2 \Phi_m \rangle_0 / \langle r^2 \rangle_0$ is lower than $1/3$, which is indicative of a negative orientational correlation between z and r.

It is interesting to note that these orientational characteristics deduced for PE are not valid for other chains. A perturbation of energy parameters in polyethylene gives rise to a substantially different orientational behavior. The motion becomes almost isotropic in model III, which is the simple chain where *trans* and *gauche* states are equally probable.

An examination of the results for asymmetric chains reveals the fact that, apart from the chemical structure, the tacticity also is an important factor to be considered when interpreting orientation measurements. Although the bond vectors are always those exhibiting the highest orientational correlation with r, their relative strength depends on the stereochemical structure of the chain. Among the model chains studied, C_{nm}/C_n values are highest for isotactic PVB and syndiotactic PVC. These chains possess the highest characteristic ratios as well. It may be easily understood that for chains with more expanded configurations, the orientational correlation between bond vectors and r is stronger. In general, vectors along the z axis of local frames exhibit negative orientation with respect to r, except for syndiotactic PVB.

In the case of chains perturbed by long-range interactions, the agreement between the results from the two sets of Monte Carlo chains is not as satisfactory as above. The D_m values are obtained from the slope of α_{sm}^2 and α_r^2 curves. The variables α_{sm}^2 and α_r^2 reflect, respectively, the change in the orientation function at fixed r, S_r, and the change in the molecular dimensions of the chains subject to long-range interactions, in comparison to unperturbed chains. In general, negative values are obtained for D_m, except for the cases where C_{nm}/C_n is very close to $1/3$, as mentioned above. This shows that α_{sm}^2 and α_r^2 change in opposite directions. Since the α_{sm}^2 vs α_r^2 curves are constrained to pass through the point $(1,1)$, it follows that $\alpha_r^2 > 1$ when $\alpha_{sm}^2 < 1$ and vice versa. Physically, this means that the expansion of the chain is accompanied by a decrease in the absolute magnitude of S_r. Thus, the chain expansion induces some disorder inasmuch as S_r approaches zero for complete disorder. In the opposite case, i.e., as the overall dimensions of the chain decrease $(\alpha_r < 1)$, the absolute magnitude of S_{cv} becomes larger than that of S_r. The tendency for orientation in a specific direction is enhanced by the decrease in the overall chain dimensions.

The long-range interactions seem to exert an isotropic effect on segmental orientation; their influence is almost the same for all directions of m within the local frame. In fact, $\langle D_x \rangle$ and $\langle D_z \rangle$ values averaged over various ranges of n for model I, are almost indistinguishable. Also the averaging over all the models with $n = 100$ yields $\langle D_x \rangle = -0.55$ and $\langle D_z \rangle = -0.56$, although the standard deviations are con-

siderably higher in this case. It is conceivable that $\langle D_y \rangle$ is nearly identical with $\langle D_x \rangle$ and $\langle D_z \rangle$, but the uncertainty in $\langle D_y \rangle$ prevents a definite statement. Nevertheless, the present analysis demonstrates that there is direct correspondence between segmental orientation and the overall chain dimensions. An increase of about 20% in α_r leads, e.g., to a decrease of 25% in the orientation function, using an average value of $\langle D_m \rangle = -0.55$.

Recently, Gao and Weiner[3] investigated the effect of a repulsive intramolecular interaction on the orientation of bond vectors, through molecular dynamics simulation of freely jointed chains. They calculated $\langle \cos^2 \theta \rangle_r$, where θ is the angle between the bond vectors and the X axis, which is identified by the end-to-end vector r. For unperturbed chains, the corresponding $\langle \cos^2 \theta \rangle_r$ is given by Eq. (6), which is exact for very long chains or when $r/nl \ll 1$, where the identification of an arbitrary axis of orientation with r is applicable.[8] For perturbed chains, $\langle \cos^2 \theta \rangle_r$ is found[3] to be smaller than $1/3$ for sufficiently small r. According to the present analysis, for chains with small r, i.e., $\alpha_r^2 < 1$, α_{sm}^2 is necessarily larger than unity, as shown in Fig. 2, and consequently S_{cv} and S_r are both positive or negative (positive for $m = x$). Thus the change in the sign of the orientation func-
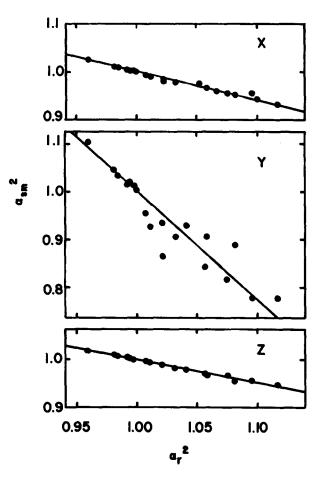

FIG. 2. Illustrative evaluation of D_x, D_y, and D_z. The data shown are for perturbed polyethylene chains with $n = 100$. The values of r^*/l are 0.6, 1.0, 1.4, and 1.8, and the values of w are 0, 0.5, 0.7, 1.04, and 1.08. The slopes of the straight lines are -0.61, -2.24, and -0.47. These three slopes are reported as D_x, D_y, and D_z, respectively, for the first simulation at $n = 100$ in Table III.

tion upon imposition of an excluded volume effect is not verified by the present work, for the central bonds of the real chains.

An approximation used in the present study is the truncation of the series in Eq. (2) after the second term. A more accurate estimation of segmental orientation, particularly in shorter chains, requires the consideration of the additional terms. However, they have been neglected here inasmuch as a major factor determining the segmental orientation is known to be the perturbation of the configurational factor as formulated in Eq. (9). It should be noted that although the perturbation of the configurational factor originated from intramolecular interactions in the present work, the results may approximately reflect the response of segmental orientation to intermolecular constraints (such as solvent effect in swollen networks or polymer–polymer interaction in concentrated systems), inasmuch as the introduced potentials give rise to some expansion or contraction of the chain, which is controlled by suitable adjustment of the parameters w and r^*/l.

[1]B. Erman and L. Monnerie, Macromolecules **18**, 1985 (1985).
[2]B. Erman and I. Bahar, Macromolecules **21**, 452 (1988).
[3]J. Gao and J. H. Weiner, Macromolecules **20**, 2520, 2525 (1987).
[4]W. L. Mattice and D. K. Carpenter, Macromolecules **17**, 625 (1984); W. L. Mattice, D. K. Carpenter, M. D. Barkley, and N. R. Kestner, *ibid.* **18**, 2236 (1985); W. L. Mattice and A. C. Lloyd, *ibid.* **19**, 2250 (1986); W. L. Mattice and E. Saiz, J. Polym. Sci. Polym. Phys. Ed. **24**, 2669 (1986).
[5]W. L. Mattice, J. Chem. Phys. **87**, 5512 (1987).
[6]K. Nagai, J. Chem. Phys. **40**, 2818 (1964).
[7]In the present treatment, the quantity $\langle r^2 \rangle^*$ defined by Nagai in Ref. 6 as $\{n \lim(\langle r^2 \rangle_0/n)\}$ is replaced by $\langle r^2 \rangle_0$, in conformity with the analogous approach used in Chap. VIII of Ref. 8.
[8]P. J. Flory, *Statistical Mechanics of Chain Molecules* (Interscience, New York, 1969).
[9]A. Abe, R. L. Jernigan, and P. J. Flory, J. Am. Chem. Soc. **88**, 631 (1966).
[10]E. Saiz, R. Riande, M. P. Delgado, and J. M. Barrales-Rienda, Macromolecules **15**, 1152 (1982).
[11]J. E. Mark, J. Chem. Phys. **56**, 451 (1972).